Open-Filter Optical SSA Analysis Considerations

John V. Lambert
Cornerstone Defense
9004 Furrow Avenue
Ellicott City, MD 21042

ABSTRACT

Optical Space Situational Awareness (SSA) sensors used for space object detection and orbit refinement measurements are typically operated in an "open-filter" mode without any spectral filters to maximize sensitivity and signal-to-noise. These same optical brightness measurements are often also employed for size determination (e.g., for orbital debris), object correlation, and object status change. These functions, especially when performed using multiple sensors, are highly dependent on sensor calibration for measurement accuracy. Open-filter SSA sensors are traditionally calibrated against the cataloged visual magnitudes of solar-type stars which have similar spectral distributions as the illuminating source, the Sun. The stellar calibration is performed to a high level of accuracy, a few hundredths of a magnitude, by observing many stars over a range of elevation angles to determine sensor, telescope, and atmospheric effects. However, space objects have individual color properties which alter the reflected solar illumination producing spectral distributions which differ from those of the calibration stars. When the stellar calibrations are applied to the space object measurements, visual magnitude values are obtained which are systematically biased. These magnitudes combined with the unknown Bond albedos of the space objects result in systematically biased size determinations which will differ between sensors. Measurements of satellites of known sizes and surface materials have been analyzed to characterize these effects. The results have combined into standardized Bond albedos to correct the measured magnitudes into object sizes. However, the actual albedo values will vary between objects and represent a mean correction subject to some uncertainty.

The objective of this discussion is to characterize the sensor spectral biases that are present in open-filter optical observations and examine the resulting brightness and albedo uncertainties that should accompany object size, correlation, or status change determinations, especially in the SSA analyses of individual space objects using data from multiple sensors.

1. BACKGROUND

Optical observations of artificial satellites began within weeks of the launch of Sputnik in 1957 with imaging from the Air Force (AF) Missile Test Center at Cape Kennedy, FL [1]. By the mid-1960s, optical observation techniques had evolved to include a broad range of advanced sensors such as electro-optical photometers and high-resolution film and television cameras designed to provide detailed information on the configuration, dynamics, and mission of the target spacecraft [2]. A number of United States Government agencies at various locations employing a variety of telescopes and instruments (see Table I) became actively involved in these operations [3].

Optical observations are divided into two types: surveillance to find objects, to obtain metric positions for orbit determination, and correlate to known objects (Detect, Track, and Identify); and Space Object Identification (SOI) for target satellite characterization. Observations from one of these missions is often processed to support the other mission. Early optical surveillance observations quickly transitioned from manual tracking using Theodolite telescopes to wide field-of-view (FoV) Baker-Nunn film cameras and still later to wide-FoV television cameras. Charge Coupled Device (CCD) cameras are now the standard, for example, the current GEODSS and SBSS sensors. These sensors are normally operated in an open-filter mode (i.e., with no spectral filters, using the full detector spectral response) to obtain maximum sensitivity. The images from these surveillance sensors are typically processed to obtain photometric magnitudes for observed satellites using the background stars as brightness references. This photometric data is used to support target correlation for closely-spaced objects, change detection (stable to unstable, orientation changes, etc.), and sizing for orbital debris objects. Early optical SOI measurements were (and still are) made using narrow-FoV tracking sensors and included photometry (open-filter, Johnson multi-color, and spectrophotometric), polarimetry, radiometry, imagery, and laser illumination (for imaging and

signatures). Mount angles and time from the narrow FoV SOI sensors could be recorded to support the surveillance mission. Both GEODSS and SBSS have auxiliary sensor options that can collect more typical SOI observations.

Table I. Early Satellite Characterization Facilities

Operational Date	Facility Name	Location	Telescope Aperture(s)
early-1960s	AF Range Measurements Laboratory Malibar Facility	Malabar, FL	1.2-m, …
1966	AF Aerospace Research Lab. Optical Properties of Orbiting Satellites (OPOS) Observatory	Wright-Paterson AFB, OH (Yellow Springs)	0.6-m
1966	NASA / Goodyear Portable Photometric Observatory	Various	0.6-m
1966	AF Avionics Laboratory Cloudcroft E-O Facility	Cloudcroft, NM	1.2, …
1966	ARPA Maui Optical Site (AMOS)	Maui, HI	1.6-m, 1.2-m, …

The early operational focus was on determining a satellite's configuration and dynamics. The primary emphasis was on open-filter measurements to achieve higher signal-to-noise ratios (SNRs) and higher temporal resolution (on the order of milliseconds) to resolve signatures and glints from rapidly moving and often tumbling Low-Earth Orbit (LEO) satellites. Additional types of measurements included multi-color, Johnson UBVRI photometry (Fig. 1), spectrophotometry, and polarimetry to better characterize the target objects and aid in the interpretation of the signatures. The observing techniques were adapted from astronomical observing and data reduction procedures including color-based transformations from instrumental to standard filter bands and frequent all-sky calibrations.

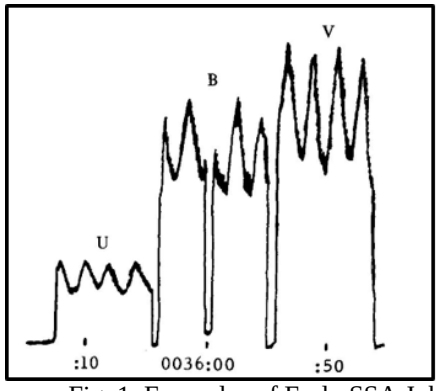

Table 2
Color indices of three balloon spacecraft as determined by five-color photometry. From ref. [30].

Color index	Reference solar value	Measured values				
		Pageos I		Echo I		Echo II
		1966	1967	1966	1967	1967
U-V	0.70	0.81	0.85	0.83	0.86	0.65
B-V	0.64	0.66	0.66	0.65	0.70	0.71
R-V	−0.52	–	−0.54	–	−0.49	−0.47
I-V	−0.78	–	−0.87	–	−0.85	−0.78

Fig. 1. Examples of Early SSA Johnson Multi-Color Observations [2]. (Right: Cosmos 192 Rocketbody, Observed on 5 Jan 1968 from ARL OPOS Observatory. Left: Balloon Satellite Observations from 1966-1967 from NASA / Goodyear Portable Photometric Observatory)

One adaptation for open-filter photometry was to reference the broadband photon count from a target to the visual "V" band magnitude of the catalogued standard stars observed for sensor calibration. Because stars of different spectral types can have the same V-magnitude but very different total broadband fluxes, a standard refinement was to restrict the reference stars to limited spectral set. That set was generally chosen to be main-sequence, G-type stars with spectra similar to the Sun. This was not because we expected the satellite to necessarily have a Solar-like spectrum, but because by narrowing the spectral diversity of the reference stars, we would have a better defined reference standard and less scatter in the calibration curves. The fact that the calibration stars matched the illumination source for the satellites was an added benefit, leaving the spectral unknowns related to the target itself. Depending on the observing situation (e.g., in-frame calibration), there might not be a sufficient number of G-type stars which are only about ten-percent of the stellar population. In these cases, reference stars from near-by types would be selected at an increase in the calibration results. This was mitigated by performing full multi-filter, all-sky calibrations of sensor several times during the night depending on conditions to track the sensor's performance for

frames with sparse stars. Variation in the selection of photometric calibration stars between sensors will result in systematic variations in reported target magnitudes and, for orbital debris observations, variations in reported sizes.

2. CURRENT SSA PHOTOMETRIC PRIORITIES

As time passed, the observing priorities for the optical non-imaging sensors shifted away from LEO to deep space (GEO, MEO, GTO, ...) observations. This shift was due to the increasing utilization of GEO for both military and civil missions; improvements in other observing techniques against LEO objects (radar and optical imaging); and because the GEO satellites were inaccessible to other techniques due to the extreme ranges. Deep space observing is well suited to optical photometric SOI sensors. Observing pass durations against are measured in hours rather than minutes, targets are available throughout the night rather than only at twilight, and illumination changes occur more slowly [4]. These factors allow the optical sensors more time for precision, multi-filter observations and to multiplex between targets improving the capability to characterize and classify satellites. The resulting improvements in photometric SOI capabilities in recent years have been documented by Payne, et al. [5].

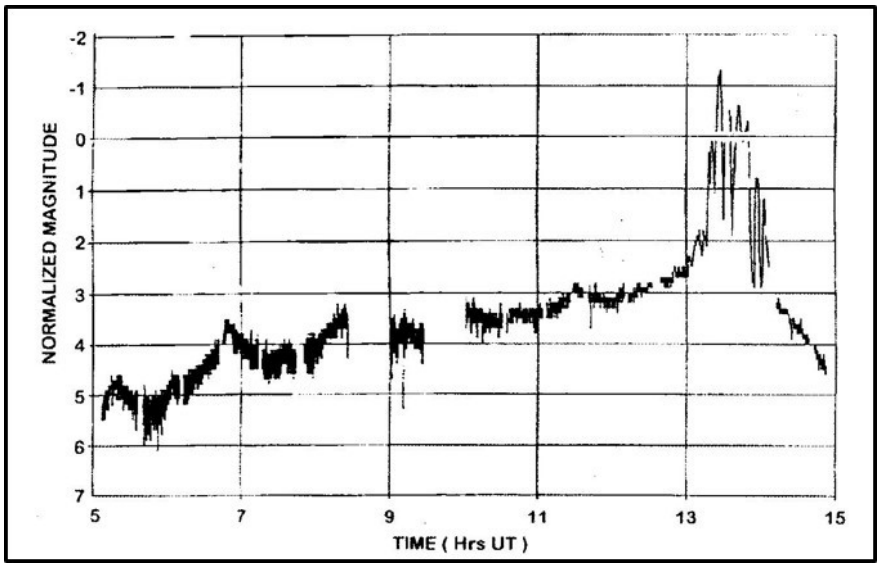

Fig. 2. Example of a Long Duration Observation of a GEO Satellite Observed from AMOS [4].

Optical surveillance sensor observing priorities have also shifted to deep space, but with other consequences. The mission requirements remain: detect, track, and identify (DTI). With the larger volume of space to monitor, the rapidly increasing number of objects to observe, and the longer ranges, surveillance sensors require maximum sensitivity and rapid coverage. The rapid coverage drives short dwell and exposure times on each target or surveillance location. Detection sensitivity and metric accuracy remain primary requirements with the SOI-related "identify" for conflict resolution and status change as secondary. The photon-starved surveillance mission cannot afford to "waste" photons with filters, so the surveillance observations are made in an open-filter mode. Open-filter observations provide the best detection sensitivity and SNR which also improves the capability to centroid the target and star positions for the best metric accuracy. The "identify" functions are still critical to overall mission success, however, and need to be made with the best possible accuracy and confidence.

A third optical SSA mission has emerged in recent years, orbital debris characterization. This mission combines elements of both of the others. It requires maximum detection sensitivity and high coverage rates, but also requires high photometric accuracy to support debris object sizing. Debris object sizing requires a Bond albedo, the broadband reflectivity, for the observed object to calculate the object's size from its observed brightness.

Open-filter surveillance is performed in one of two modes: rate track where the sensor follows the expected motion of the target(s), or sidereal track where the sensor follows the background stars. Rate track provides the best detection sensitivity by concentrating all of the target's photons on a few pixels. However, detection sensitivity is

decreased for any other targets in the field-of-view that have different motions. Sidereal track is typically used for broad-area coverage. For specific types of coverage, e.g. geosynchronous-belt searches, rate track may be used.

3. SATELLITE PHOTOMETRY

The selection of open-filter reference stars and the (unknown) spectra of individual target objects will affect the accuracy of the photometry for individual satellites and the inter-comparability of observations between sensors. For orbital observations, consistent calibration techniques are required for characterization of detected objects and for application of albedos determined by other sensor and/or based on observations of other objects. The variation in the spectra between individual objects is a limitation in open-filter observations that affects the computed magnitudes. Each type of satellite has a unique reflectance spectrum based on the combination and configuration of different surfaces and that unique spectrum can vary dramatically with the illumination geometry.

Examples of the variation in component spectra are shown in Figs. 3 and 4 which show the observed spectra from satellites when the spectra are dominated by particular surfaces. Fig. 3 shows the moderate-resolution (150Å) spectra from two types of LEO rocketbodies compared to the spectrum of zinc oxide, a common white paint pigment [6]. Object 3819 is the Soviet upper stage used to launch Cosmos 272 on 17 March 1969. Object 4392 is the People's Republic of China (PRC) upper stage used to launch the first PRC satellite (Dongfanghong I, "The East Is Red") on 24 April 1970. Neither object is still in orbit. The difference between the spectra of the two objects is most likely due to the actual pigments and binders used in their paints. The most conspicuous features of these spectra is the high, almost flat reflectance through most of the visible spectrum and the sharp falloff at short wave lengths around 4000Å (blue). The reflectance spectra of bare aluminum surfaces and metallic foils is similar. This will result in the colors of these objects appearing redder than the Sun and, depending on the sensor spectral response, fainter than would be observed with a sensor with uniform response.

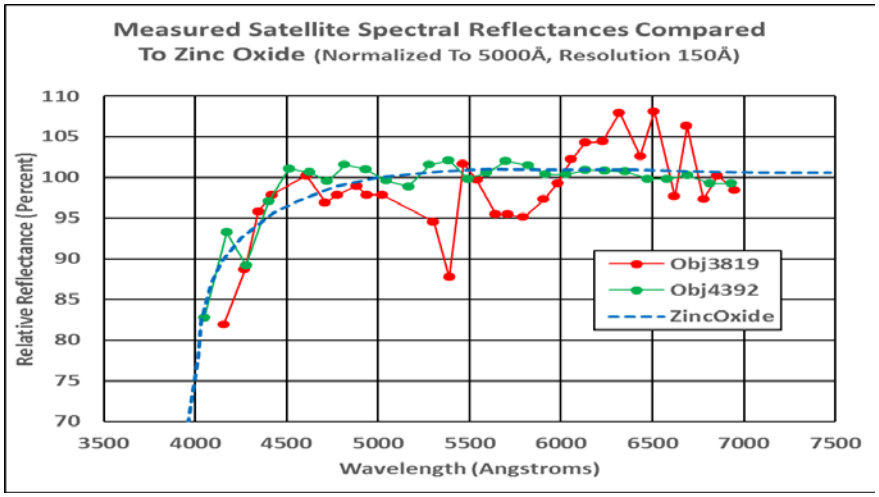

Fig. 3. Observed LEO Rocketbody Spectra [6].

Fig. 4 shows the observed high-resolution (6Å) spectrum of solar panel glints from a geosynchronous satellite [7]. The spectrophotometer was manually gated to collect data only at the peaks of the specular glints from this satellite. This spectrum is almost the inverse of the previous spectrum displaying low reflectivity throughout most of the visible region and high reflectivity in the blue around 4000Å. Satellite spectra at this resolution offer the added capability not only to identify a reflecting surface as a solar panel, but can also identify the specific type of material, possibly to its manufacturer. The small peak near 4600Å, for example, is unique to certain types of solar cells. References [8] and [9] contain additional examples and analysis of observed spectra of on-orbit satellites.

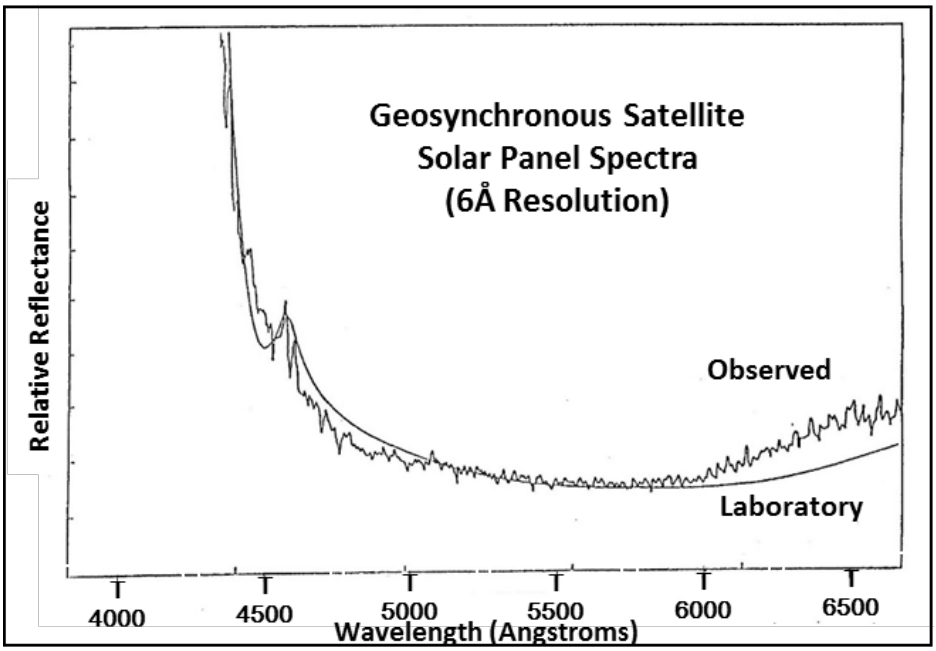

Fig. 4. Observed GEO Satellite Glint Spectrum [7].

Fig. 5 demonstrates the color changes that result as different surfaces on a GEO satellite are illuminated [5]. As the observation progresses, the spectrum is first dominated by the spacecraft body (which is redder than the sun), then by solar panels (which are bluer), then back to the body. As a satellite changes color, its observed open-filter magnitude will change non-linearly relative to the reference star calibration making comparisons to earlier observations more difficult and less consistent. These results are in agreement with the previous spectra plots.

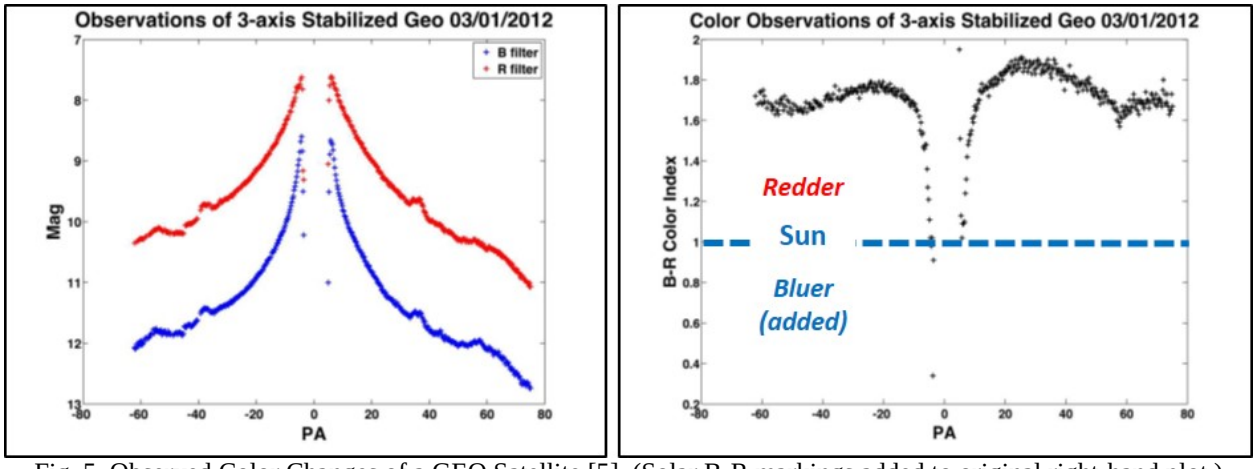

Fig. 5. Observed Color Changes of a GEO Satellite [5]. (Solar B-R markings added to original right-hand plot.)

One advantage of open-filter observations is that they capture the spectrum of a satellite over a much broader spectral range than standard color band observations so the computed Bond albedos are less likely to be biased by localized spectral peculiarities. Some results of the application of open-filter observations to orbital debris sizing are shown in Fig. 6. While most debris albedo calculations are based on comparisons of radar and optical sizing, these open-filter, optical-only results utilized a comparison between visible and thermal infrared observations [10]. Multiple observations of three objects are joined by lines. While two of them are reasonably consistent, one does show a possible variation between object surfaces. Further analysis of these data yielded a mean albedo of 0.14 [12]. Comparison of these optical results with available radar-based results [11] in Fig. 6 shows a fair agreement with perhaps an interesting deviation at larger radar sizes. The differences may be due to high dependence on the albedo

in the visible-infrared analysis leading to more sensitivity to the surface properties. Further investigation of this technique for optical determination of orbital debris albedos and diameters may be warranted.

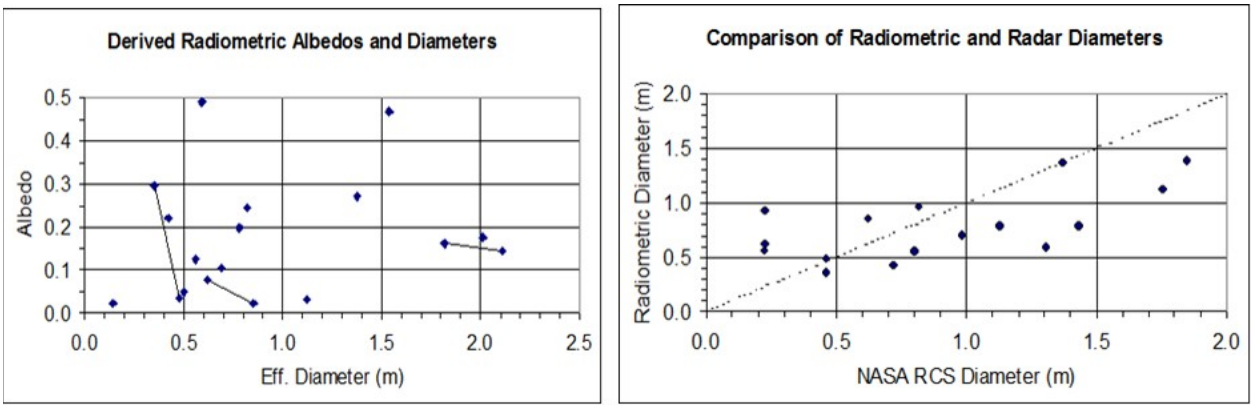

Fig. 6. Orbital Debris Albedos and Diameters Derived from Visible and Thermal Infrared Radiometry (Left); Comparison of Optical and Radar Diameters (Right). [10]

The major application of open-filter optical photometry to orbital debris analyses has been to determine an average albedo from analysis of optical and radar observations of larger objects that can then be utilized in sizing calculations from optical open-filter only observations. Especially in deep space, a region of high interest, optical observations of smaller objects are far more plentiful than radar observations. The frequency distributions of size with number of objects are then used to determine debris population distributions used in, for example, spacecraft hazard calculations [11, 12]. These average albedos are also frequently used to estimate performance in terms of detectable target size of actual or proposed optical SSA sensors against targets at given ranges. The average albedos are usually reported as specific values (i.e., 0.14) with not estimates of the uncertainty provided whether due to measurement or modelling errors. Estimates of the uncertainties would be helpful and could be calculated from the scatter in derived albedo-diameter plots.

The various spacecraft materials have different albedos [14]. It has been noted that the computed albedos of debris objects tend to cluster [12] perhaps as a function of their surface material properties. Jorgensen [8], for example, examined the potential for grouping satellite reflectance properties into categories based on their reflectance spectra. Systematic differences in albedos have been identified for large versus small objects and might be attributed to possible mixtures of materials on larger objects. One reason for the lack of separation to computed albedos might be due to the estimate that the majority of debris objects are aluminum [8]. Perhaps as more observations become available, separation of albedos due to differing material composition may emerge. This would be significant since the mass of a debris object, a contributor to its projected collision hazard, is a function of the density of its material type.

4. Proposed Open-Filter Photometric Improvements

Payne, et al. [5] have documented approaches to improving multi-color SSA photometry based on current astronomical advancements. While astronomical photometry is a true art form capable of delivering highly accurate results for many SSA applications, broadband, open-filter photometry satisfies operational SSA mission requirements for detection sensitivity and high paced observations so will remain a standard observing technique. However, improvements to the manner in which open-filter observations are collected are possible and will improve their mission utility. The simplest is to document and publish descriptions of the manner in which the various SSA sensors are calibrated and collect their measurements leading to an understanding of the commonalities and differences and improved utilization of the data and intercomparison of the results. If significant differences in the observational techniques are found between sensors, the next step would be to move toward a common methodology and examine previously collected data for possible reprocessing to a common schema.

Stars with the same V-band (or other photometric band) magnitude will have different total broadband fluxes depending on their spectral type (i.e., temperature, colors, etc.). This will cause systematic calibration uncertainties depending on the selection of calibration stars. One approach, restricting calibration stars to a narrow range of spectral types, e.g. G-type stars, reduces some of the induced scatter, but night-to-night or seasonal variations in the

calibration star sets and limited availability of stars for in-frame calibration will produce variations in the calibration results. A potential improvement to open-filter is to adopt a stellar calibration reference system that is more consistent with the very wide spectral band than the current Johnson V-band magnitude reference. Since the spectral distributions of the light reflected from satellites do not match those of the calibration stars, direct application of the open-filter stellar calibration results to the satellite open-filter measurements will result in differences in the derived fluxes. Careful application of the results of detailed in-situ and laboratory characterizations (spectra, colors, albedos, etc.) of selected satellites and satellite materials is necessary. The spectral differences between satellites and stars affects the determination of even a basic calibration parameter, atmospheric extinction (absorption and scattering). Astronomical photometric calibration includes a color term, e.g., B-V, to account for the higher extinction in the blue. If the color of a satellite is not known or estimated, use of the extinction from the stellar calibrations can result in a systematic variation of magnitude with elevation angle.

One possible improvement to the stellar photometric calibration might be a transition to the ultra-broadband filters and reference stars employed in the Sloan and Hipparcos survey systems which have wider passbands than the Johnson UBVRI broadband system [15]. (This reference also provides an excellent overview of the history and the considerations in establishing a standard photometric system.) Astronomical survey sensors share many of the requirements of SSA surveillance sensors such as detection sensitivity, wide-area coverage, and short dwell times. The passbands are designed less to capture specific low-level features in stellar spectra and more to support rapid, not overly detailed classification. Referencing measurements to an ultra-broad band in the visible for calibration should provide a better reference for open-filter SSA measurements and open the selection of reference stars to a wider range of spectral types.

Along these same lines, open-filter SSA sensors could develop a full visible-spectrum photometric system anchored to a standard astronomical photometric system. A number of mathematical expressions exist for calculating the effective blackbody temperature of a star from photometric colors. One of the simplest is the Ballesteros algorithm [16]:

$$\text{Temp } (^\circ\text{K}) = 4600 \{1/[0.92*(\text{B-V}) + 1.7] + 1/[0.92*(\text{B-V}) + 0.62]\}$$

Inserting this temperature into the Plank function will yield an effective broadband spectral distribution for a reference star, less spectral absorption lines, etc. (Fig.7). Integrating this distribution convolved with the spectral response of a standard or typical CCD (and perhaps a standard atmospheric spectral transmission if the CCD response is wide enough) will yield a full-spectrum response function for that star that could serve as a better reference for open-filter SSA observations. A bright, well-calibrated solar-type star closely matching the Sun could be selected as the zero-magnitude standard.

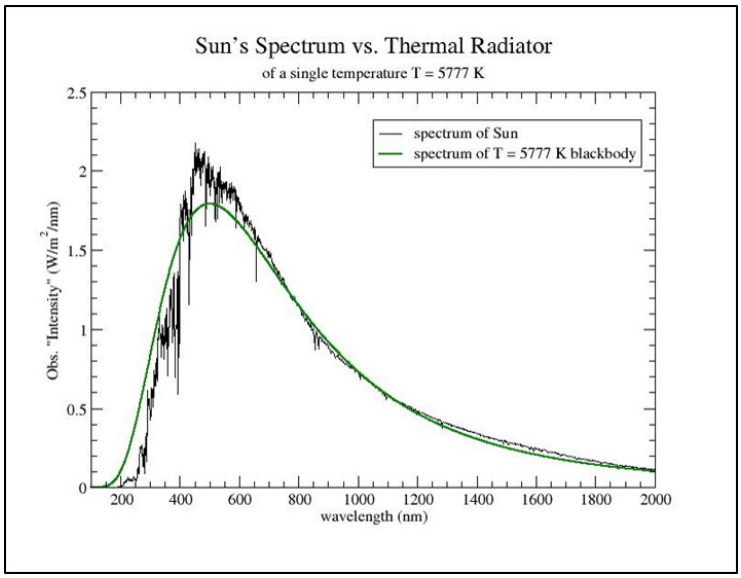

Fig. 7. Comparison Of Solar And Blackbody Spectra [17].

This system would not require extensive re-surveys of thousands of stars to establish reference standards since the Johnson, Sloan, or other photometric system colors from existing stellar catalogs already exist. Most CCDs have fairly similar spectral responses so it should be possible to compute transforms from this broadband system to sensor systems using other CCDs, again using catalogued standard photometric system colors. Transformations from a sensor's instrumental magnitudes to the defined standard photometric system magnitudes are standard with every astronomical sensor already. This approach ignores the finer details of stellar spectral, but that should have a small impact over the entire visible spectral range. The stellar calibration uncertainties will be large compared to astronomical standards, but should be more consistent than current SSA open-filter approaches referenced only to stellar V-band magnitudes and would definitely allow the use of a wider range of spectral types for calibration. A test of this approach should be straightforward with existing SSA or astronomical sensors.

5. References

1. Duke, D. and Kissell, K.E. *Proceedings of University of Miami Symposium on Optical Properties of Orbiting Satellites*. Aerospace Research Laboratories, Wright-Patterson AFB, OH. 1969.
2. Kissell, K.E. *Diagnosis of Spacecraft Surface Properties and Dynamical Motions by Optical Photometry*. (ARL 69-0082). USAF Office of Aerospace Research / Aerospace Research Laboratory, Wright-Patterson AFB, OH.1969. (Reprinted from *Space Research IX*, North-Holland Publishing Company, Amsterdam. 1969.)
3. Lambert, J.V. and Kissell, K.E. The Early Development of Satellite Characterization Capabilities at the Air Force Laboratories. In *2006 AMOS Technical Conference*, Maui, HI. 2006.
4. Lambert, J.V. Motion and Configuration from Optical Signatures. Internal Memo. 2001.
5. Payne, T.E., Castro, P.J., Gregory, S.A., and Dao, P. Satellite Photometric Error Determination. In *2015 AMOS Technical Conference*, Maui, HI. 2015.
6. Lambert, J.V. *Measurement of the Visible Reflectance Spectra of Orbiting Satellites*. M.S. Thesis, GEP/PH/71-11. Air Force Institute of Technology. Wright-Patterson AFB, OH. 1971.
7. Lambert, J.V. and Mavko, G.E. Spectrophotometric Signatures of Synchronous Satellites. *Proceedings of NORSIC-7* (NORAD Spacecraft Identification Conference). Air Force Academy, Colorado Springs. 1975.
8. Lambert, J.V., Osteen, T.J., and Kraszewski, W.A. Determination of Debris Albedo from Visible and Infrared Brightnesses. *Proceedings of SPIE's OE/Aerospace and Remote Sensing Symposium*. 1993.
9. Jorgensen, K.M. *Using Reflectance Spectroscopy to Determine Material Type of Orbital Debris*. Ph.D. Thesis. University of Colorado, Boulder, CO. 2000.
10. Seitzer, P., Lederer, S.M., Cowardin, H., Cardona, T., Barker, E.S., Abercromby, K.J. Visible Light Spectra of GEO Debris. In *2012 AMOS Technical Conference*, Maui, HI. 2012.
11. Henize, K.G., O'Neill, C.A., Mulrooney, M.K., and Anz-Meador, P. Optical Properties of Orbital Debris. Submitted to *Journal of Spacecraft and Rockets*. 1993. (Published Vol. 31, No. 4, July-August 1994.)
12. Kessler, D.J., and Jarvis, K.S. Obtaining The Properly Weighted Average Albedo of Orbital Debris from Optical and Radar Data. *Advances in Space Research*, Volume 34, Issue 5, p. 1006-1012. 2004.
13. Mulrooney, M.K. and Matney, M.J. Derivation and Application of a Global Albedo Yielding an Optical Brightness to Physical Size Transformation Free of Systematic Errors. In *2007 AMOS Technical Conference*, Maui, HI. 2007.
14. Hejduk, M.D., Cowardin, H.M., and Stansbery, E.G. Satellite Material Type and Phase Function Determination in Support of Orbital Debris Size Estimation. In *2012 AMOS Technical Conference*, Maui, HI. 2012.
15. Bessell, M.S. Standard Photometric Systems. *Annual Review of Astronomy and Astrophysics 43*. 2005.
16. Balesteros, F.J. New Insights Into Blackbodies. http://arxiv.org/pdf/1201.1809.pdf 2012.
17. Korista, K. *Physics 3250: Introduction to Astrophysics…Spring 2016*. Western Michigan University. 2016. (http://homepages.wmich.edu/~korista/phys3250.html)